ASTM INTERNATIONAL

Journal of Testing and Evaluation

Ane C. Rovani,[1] Tiago A. Rosso,[1] and Giuseppe Pintaude[2]

DOI: 10.1520/JTE20180576

On the Use of Microscale Abrasion Test for Determining the Particle Abrasivity

Journal of Testing and Evaluation

doi:10.1520/JTE20180576 available online at www.astm.org

Ane C. Rovani,[1] Tiago A. Rosso,[1] and Giuseppe Pintaude[2]

On the Use of Microscale Abrasion Test for Determining the Particle Abrasivity

Reference

A. C. Rovani, T. A. Rosso, and G. Pintaude, "On the Use of Microscale Abrasion Test for Determining the Particle Abrasivity," *Journal of Testing and Evaluation* https://doi.org/10.1520/JTE20180576

ABSTRACT

Particle abrasivity is an important concept for helping to select materials for pumps and for disc cutters in underground excavation, and specific ASTM standards are available for making these selections. However, for manufacturing processes in which abrasive action is their core, the particle size range is approximately a few micrometers. The evaluation of particle abrasivity using the microscale abrasion test matches this range of particles for this purpose, but relatively few investigations using this kind of method have been conducted. The aim of this investigation is to use the microscale abrasion test to evaluate the particle abrasivity, avoiding changes on the ball surface and on the particle size distribution. Samples of quenched AISI D2 tool steel were used for tests. The wear mode was dependent on the testing time. Alumina (Al_2O_3) particles presented a lower abrasiveness when compared to boron carbide (B_4C) ones, confirmed by the higher wear coefficient found in the latter after reaching the steady-state regime. This behavior was evidenced by the number of active particles in the contact, which showed that there were a larger number of B_4C particles than Al_2O_3 during the contact at all sliding distances. The particle abrasivity is discussed in terms of significant characteristics of slurries: particle shape, particle size distribution, hardness-to-elastic modulus ratio, zeta potential, and density. As the controlling of those characteristics seems to be very important, particle abrasivity is a concept that needs to be improved besides the test system used for that purpose.

Keywords

abrasiveness, micro-abrasive wear, abrasive particles, alumina, boron carbide

Manuscript received August 9, 2018; accepted for publication February 19, 2019; published online May 8, 2019.

[1] Academic Department of Mechanics, Surface and Contact Lab (LASC), Universidade Tecnológica Federal do Paraná, Rua Deputado Heitor Alencar Furtado, 5000, Curitiba 81280-340, Brazil, http://orcid.org/0000-0002-6042-6607 (A.C.R.)

[2] Academic Department of Mechanics, Surface and Contact Lab (LASC), Universidade Tecnológica Federal do Paraná, Rua Deputado Heitor Alencar Furtado, 5000, Curitiba 81280-340, Brazil (Corresponding author), e-mail: giuseppepintaude@gmail.com, http://orcid.org/0000-0001-8215-4481

Introduction

The term "abrasivity" can be defined as the potential of a rock or soil to cause wear on a tool.[1] Concerning this definition, two ASTM standards have been used in intense

industrial application: ASTM G75, *Standard Test Method for Determination of Slurry Abrasivity (Miller Number) and Slurry Abrasion Response of Materials (SAR Number)*[2] and ASTM D7625, *Standard Test Method for Laboratory Determination of Abrasiveness of Rock Using the CERCHAR Method*,[3] Miller number and Cherchar abrasiveness index (CAI), respectively. The Miller number can be used for helping with the materials selection for pumps, whereas the CAI is related to the performance of disc cutters in underground excavation.[4] These methods have a similar aspect regarding the use of a reference material: the Miller number is determined for 27 % chromium iron, whereas the CAI requires a stylus with a hardness value of 55 HRC for every test.

Some tests aimed at determining the abrasive wear resistance of materials have also been used for checking the particle abrasivity, such as the jaw crusher gouging abrasion test outlined in ASTM G81, *Standard Test Method for Jaw Crusher Gouging Abrasion Test*.[5] In this system, Pintaude and Bartalini[6] verified a significant influence of the quartz content on the abrasivity of rocks. Typical average sizes of particles used for the gouging abrasion test are of some millimeters, which is much bigger than those used for abrasive machining. On the other hand, in the microscale abrasion test ISO 26424:2008, *Fine Ceramics (Advanced Ceramics, Advanced Technical Ceramics) — Determination of the Abrasion Resistance of Coatings by a Microscale Abrasion Test*,[7] the particles are of the order of some micrometers, which is equivalent to the range of sizes commonly found for manufacturing.[8] In the same fashion as that noted for the gouging abrasion test, some investigations already made use of the microscale abrasion test to determine the particle abrasivity, although it is preferable to use it for determining the thickness and the wear resistance of coatings.[9]

Kelly and Hutchings[10] proposed a method to measure the abrasiveness of particles, modifying the microscale abrasion test configuration (fixed ball). They proposed a contact between a fixed cylindrical nylon disc—instead of a ball—and a plane specimen of PMMA, which serves as a reference material. The tested abrasives varied from 2.39 to 152 μm, which is a wider range of particle sizes than those usually verified in the more conventional ball-cratering method.

Following the idea to extend the range of particle sizes, Stachowiak and Stachowiak[11] evaluated the influence of the abrasive particles (glass beads, silica sand, quartz, and alumina [Al_2O_3]) on the wear rates of mild steel and 27 % chromium white cast iron. The tests were performed in a free-ball configuration. Probably the main differences in the testing variables used by Stachowiak and Stachowiak from those described in ISO 26424:20087 were the applied load of 1.4 N and the diameter of 41.3 mm of the bearing ball.[11] With these conditions, they found that the particles fracture during the test, meaning that the imposed conditions gave rise to a high-stress abrasion under the operating conditions used.

In both investigations, the particle size distribution was not described. A further study proves that the mean average size of particles is not enough to guarantee a constant particle size effect on the wear results.[12]

Significant efforts were made to promote a standardization of the microscale abrasion test.[13] Some parameters are discussed, such as the particle size, shape, and material of abrasives, the type of suspension fluid, the load, the speed, and the ball material and its surface condition. Among them, the sliding speed, an important parameter, was mentioned. Results showed that the increase of sliding speed (from 0.02 to 0.14 m/s) can reduce the wear rate. However, this decreasing can be associated with uncertainty with the drive shaft because the free-ball system is driven by the friction between the ball and de-drive shaft.[13]

Even though this round-robin evaluation had led to the conception of an ISO standard, the effect of sliding speed is not a consensus. For example, Bello and Wood[14] found an increase in the wear coefficient as the sliding speed was increased. They justified this effect by the creation of a hydrodynamic layer, which would reduce the interaction between the specimen and the particles, giving rise to a decrease in the wear volume.

From the presented findings of the literature, this study aims at evaluating the particle abrasivity using the microscale abrasion test, considering the possibilities of avoiding the effect of the size and shape of particles, avoiding their fracture, and causing a minimum change on the ball surface roughness.

Experimental Procedure

SAMPLES AND CHARACTERIZATION

The material used for the experiments was AISI D2 tool steel, quenched and tempered according to ASTM G65, *Standard Test Method for Measuring Abrasion Using the Dry Sand/Rubber Wheel*[15] (austenitizing at 1,010°C for 25 min. following air-cooling). This steel was selected with the purpose of evaluating the abrasivity because of the easy reproducibility of the heat treatment and because of its well-reported values of hardness (58–60 HRC, ASTM G65). The hardness measurements of the samples were carried out in Shimadzu HMV-2 equipment. The average values corresponded to a series of five measurements, resulting in 677 ± 9 $HV_{0.1}$ (or 59.1 ± 0.4 HRC).

ABRASIVE PARTICLES

Two kinds of abrasives materials were tested: Al_2O_3 and boron carbide (B_4C). Al_2O_3 is a standard abrasive indicated by ISO 26424:20066 for the microscale abrasion test. On the other hand, B_4C is applicable for specific industrial processes, such as the hydro-erosive grinding.[16]

The particle size distribution of abrasive materials was determined using the laser diffraction method, a Microtrac brand granulometer, model S3500, with detection limit sizes between 0.02 and 2,800 μm. Isopropyl alcohol was used as a dispersing medium.

The particle size distributions of B_4C and Al_2O_3 are shown in **figure 1*A*** in the form of a frequency distribution by volume and in **figure 1*B*** as cumulative frequency. One can observe that any significant difference exists between two abrasive materials, being that this variable can be considered as a constant.

The particle geometries were characterized using the quadratic adjustment tip parameter, Spike Parameter–Quadratic fit (SPQ). This parameter was determined using a computational tool presented in Coseglio et al. (2015).[16] For each abrasive material, twenty random particles were analyzed, in which their images were obtained in a scanning electron microscope (SEM), as shown in **figure 2**.

The SPQ values are presented in **Table 1**. The separation of values at a diameter of 7 μm is used to compare the values with those obtained in ASTM G65-16e1[15] for the B_4C.

For particles greater than 7 μm, we found similar values of SPQ in relation with those presented in ASTM G65-16e1,[15] even with lower deviations. One can consider the SPQ of Al_2O_3 to be equally similar to those determined for the B_4C. On the other hand, Coseglio et al.[16] found higher values of SPQ for particles less than 7 μm of B_4C, whereas in this investigation, the values for B_4C and Al_2O_3 can be considered as being equal. The differences found among the SPQ values of B_4C can indicate a dependence on the size of sampling for determining the SPQ, which to our knowledge, there is no detailed study of this at the moment. As discussed in detail by Pintaude,[17] differences in the particle size cannot be used to explain any differences in the particle shape. As an example, Pintaude and Coseglio[18] found for twenty particles of Al_2O_3, whose average sizes were 360 ± 50 μm, an SPQ of 0.37 ± 0.15, which is a value very close to that presented in **Table 1**.

Despite this discussion, we will consider the particle shape of tested abrasive materials to be a constant, in a similar way that was found for the particle size distribution.

Additionally, the number of active particles between the ball and the specimen was determined using equation (1) according to Adachi and Hutchings.[19] The number of active particles was considered using the mean values of particle diameters obtained according to **figure 1**.

$$N = \frac{Ac\upsilon}{\pi * D^2} \tag{1}$$

where:

N = number of particles in contact,
Ac = apparent contact area,
υ = volume fraction of abrasive, and
D = mean particle diameter.

FIG. 1

(*A*) Distribution of particle size frequency by volume. (*B*) Cumulative volume particle size frequency for B_4C and Al_2O_3.

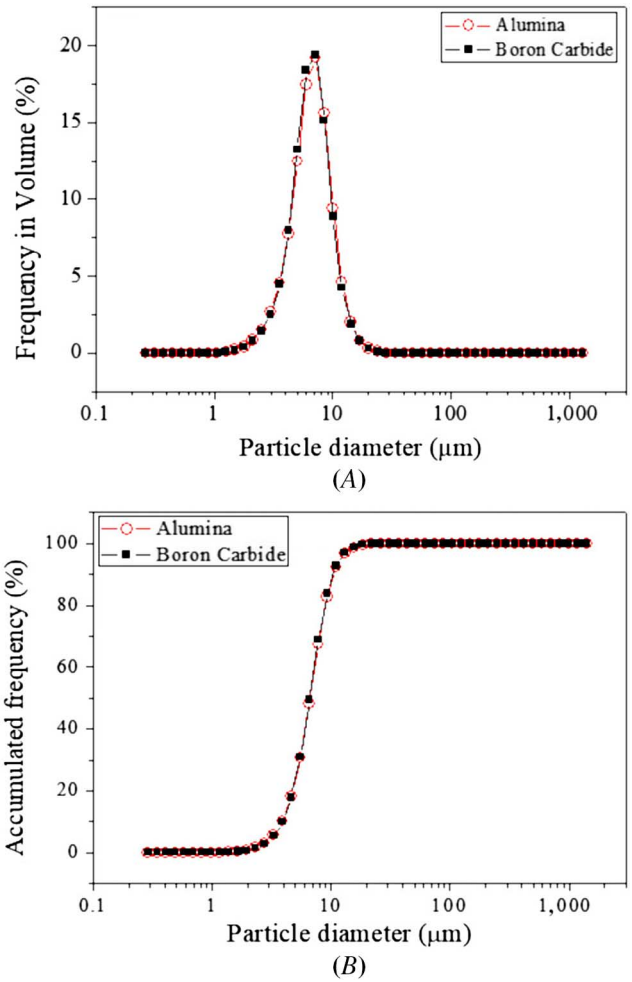

MICROSCALE ABRASION TESTS

The abrasiveness tests carried out in a compact Calotest (Cat2). Tests were performed with a steel ball with a diameter of 25.4 mm and with a hardness of 716 ± 9 $HV_{0.1}$. The roughness of the ball in the initial state was $Sq = 0.05 \pm 0.01$ μm without any kind of preconditioning. Table 2 shows the parameters used for the tests. The average values of crater diameters correspond to a series of three repetitions.

The diameters of craters were measured by optical microscopy, and the wear mechanisms were evaluated in an SEM.

The wear coefficient (k) was calculated according equation (2).

$$k = \frac{d^4}{128NR^2tn} \tag{2}$$

where:

d = diameter of wear crater (mm),
N = applied load (N),
t = time of the test (s), and
n = rotations of the ball (rpm).

FIG. 2 SEM image for SPQ calculation (B_4C).

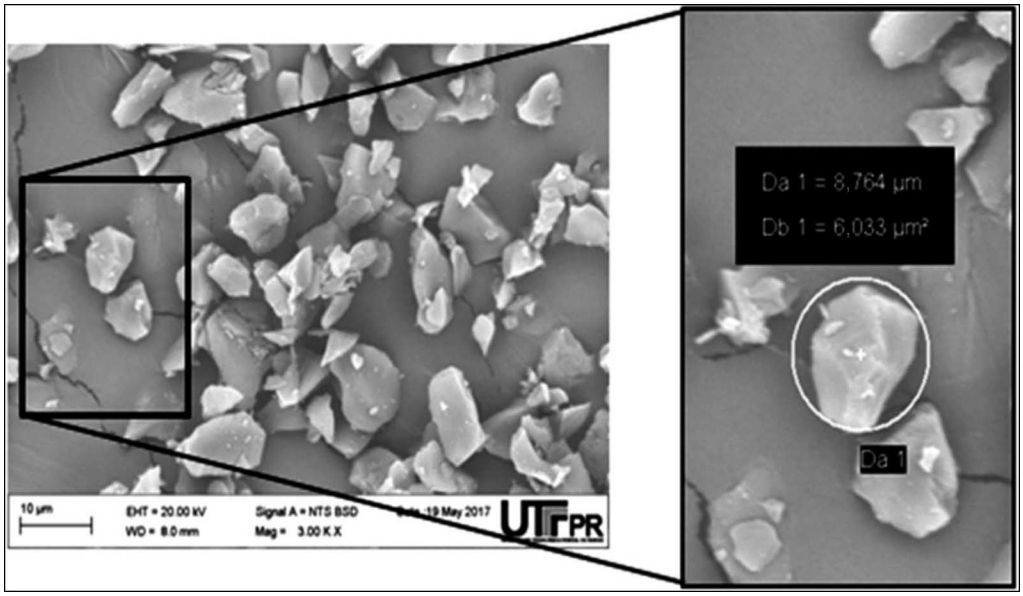

TABLE 1
Values of SPQ parameter

	B_4C	B_4C[15]	Al_2O_3
Particles $d > 7$ µm	0.34 ± 0.11	0.4 ± 0.2	0.44 ± 0.09
Particles $d < 7$ µm	0.44 ± 0.14	0.7 ± 0.1	0.40 ± 0.11

TABLE 2
Testing parameters used for abrasiveness evaluation

Parameters	Conditions
Axis rotation, rpm	300
Ball rotational speed, rpm	190
Angle, °	30
Sliding distance, m	48, 96, 192, 287, 383, 575, 766
Load, N	0.27
Abrasive concentration	10 % Vol.
Abrasive slurry supply	1 drop/15 s

For the crater's profile characterization, a Talysurf CCI Lite Noncontact 3-D Profilometer was used. Sq amplitude and $S\Delta q$ hybrid roughness parameters were determined. The parameter $S\Delta q$ represents the mean square slope of the profile. The parameter λq, obtained through equation (3), can represent the width of the wear caused by the abrasive particles.[20] **Figure 3** represents the profile of the roughness measurement inside the wear crater.

$$\lambda_q = \frac{2\pi S_q}{S_{\Delta q}} \tag{3}$$

FIG. 3 Profile of the worn crater with B_4C abrasive for 96 m of sliding distance.

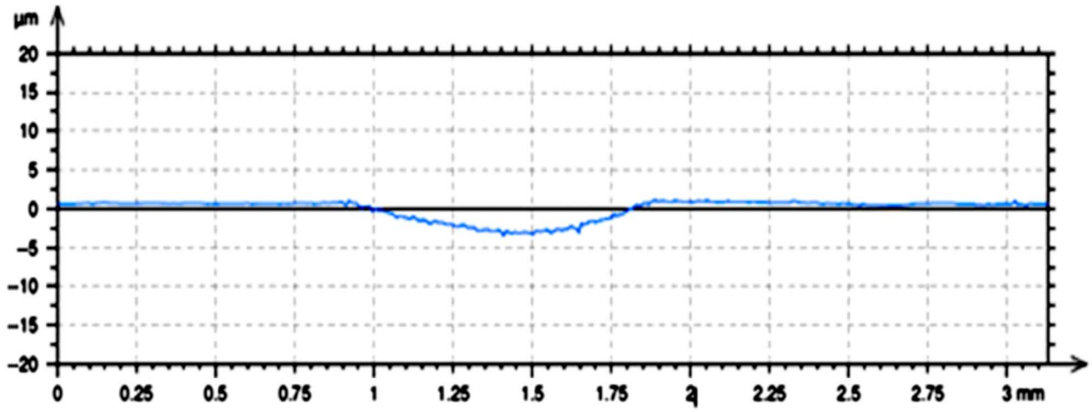

Results and Discussion

WEAR COEFFICIENT AND WORN SURFACES

Figure 4 shows the wear coefficient as a function of the sliding distance. It was observed that the steady-state of wear, in terms of the sliding distance, was not the same for both of the abrasive materials used.

The wear coefficient increased with the sliding distance until it reached the steady-state. For Al_2O_3, the steady-state was observed with 192 m of sliding distance, whereas for B_4C, the steady-state was observed with 383 m of sliding distance. Before the transition period was observed, the wear coefficient presented different behavior when compared with the period after the transition from the wear regime. For the B_4C, the wear coefficient was lower than for Al_2O_3, before the steady-state. After the steady-state, it was observed that the wear coefficient of the B_4C was higher when compared to the Al_2O_3.

To understand the changes that occurred on the wear surface and the wear mechanisms before, during, and after the steady-state, the surface was analyzed at the sliding distance of 96, 192, 287, and 383 m; these are the sliding distances that covered the wear transition period for both abrasives. Figure 5 shows the wear surface with B_4C abrasive to the condition of 96 m (fig. 5*A*), 192 m (fig. 5*B*), 287 m (fig. 5*C*), and 383 m (fig. 5*D*).

FIG. 4

Wear coefficient as a function of the sliding distance.

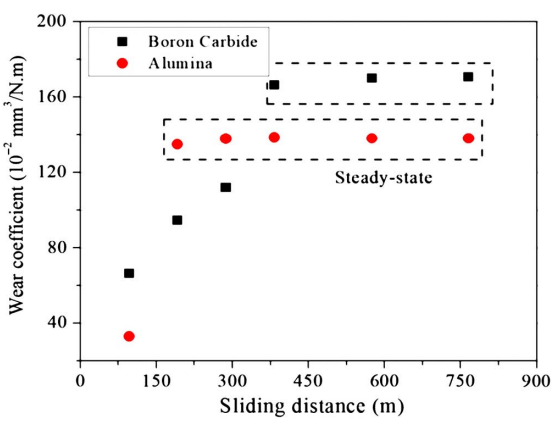

Two kinds of wear modes were observed. Before the steady-state regime, a mixed behavior between rolling and grooving wear can be observed. According to Allsopp and Hutchings,[21] the abrasive particles are not embedded but roll between the two surfaces, producing a heavily deformed, multiply indented wear surface with no evident surface directionality. Finally, for the 383 m of sliding distance (**fig. 5*D***), the wear mode presented is grooving, where there is a continuous direction of the grooves and the steady-state is observed.[22]

Similarly, using Al_2O_3 as an abrasive, according to **figure 6**, before the steady-state regime, the wear mode was mixed at 96 m (**fig. 6*A***), followed by grooving mode of wear after 96 m (**fig. 6*B–D***).

The wear marks for the B_4C show more accentuation and show a higher value of the wear coefficient, according to **figure 4**.

Table 3 presents the values of S_q and λ_q parameters for the worn surfaces by the B_4C and Al_2O_3 abrasives. The increased sliding distance causes an increase in the *Sq* parameter. In addition, the values promoted by the wear caused by the B_4C were higher than those determined in the case of the Al_2O_3, which is proportional to the higher wear coefficients already described.

On the other hand, the λ_q value allows for another view of the wear process because the value of *Sq* is included in it. First of all, the difference between the λ_q value caused by the B_4C and those caused by the Al_2O_3 is not as large as the difference noted for the *Sq* parameter. Finally, as the sliding distance increased, there was a stabilization on the λ_q values, indicating that the width of the wear tracks (inside the crater) remained constant for a certain period of the test.

For the tests with B_4C, the value of the parameter λ_q shown in **Table 3** presented a reduction in the value from 287 m of sliding distance when a transition of wear modes occurred. For the Al_2O_3, the value of this

FIG. 5 Worn surfaces after test with abrasive particles of B_4C for tests with (*A*) 96 m, (*B*)192 m, (*C*) 287 m and (*D*) 383 m.

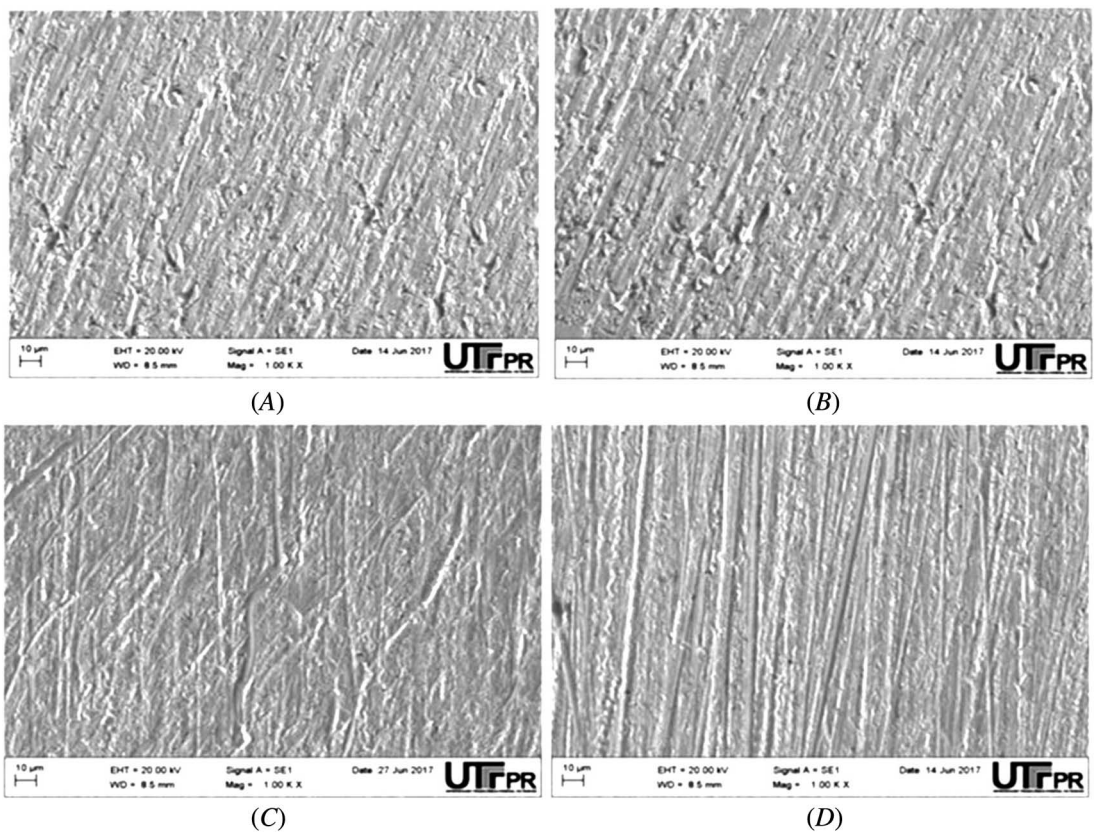

FIG. 6 Worn surfaces after tests with abrasive particles of Al_2O_3 for tests with (*A*) 96 m, (*B*) 192 m, (*C*) 287 m, and (*D*) 383 m.

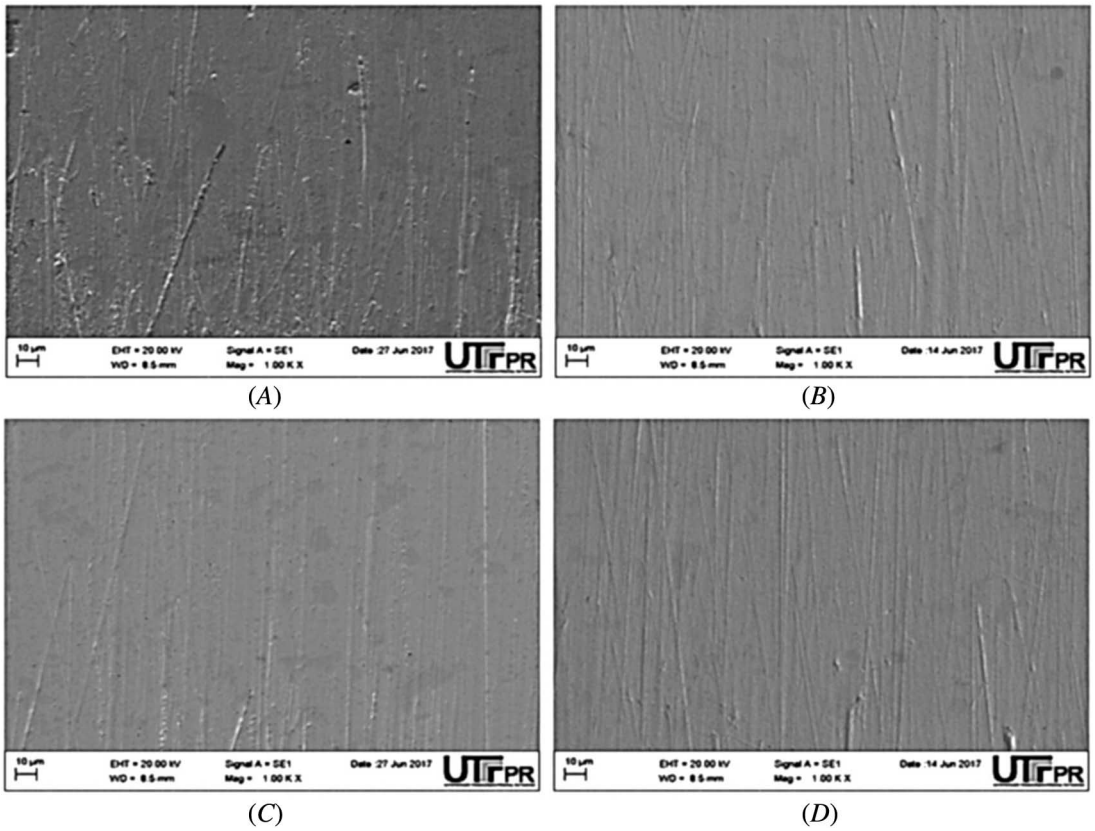

TABLE 3
Sq and λ_q roughness parameter of worn surfaces to B_4C and Al_2O_3

	B_4C		Al_2O_3	
Sliding distance, m	S_q, μm	λ_q	S_q, μm	λ_q
96	0.12 ± 0.01	27.1 ± 0.2	0.06 ± 0.01	32.9 ± 0.5
192	0.13 ± 0.01	27.7 ± 0.3	0.06 ± 0.01	24.7 ± 0.5
287	0.18 ± 0.02	17.9 ± 0.3	0.05 ± 0.01	25.0 ± 0.5
383	0.24 ± 0.03	15.1 ± 0.3	0.11 ± 0.01	24.5 ± 0.5

parameter presented a smaller value for the tests after 192 m. Because this parameter represents the approximate width of the wear groove caused by a particle, it can be inferred that when the permanent regime is reached, we have a probable value of the wear width for such conditions and a probable stabilization thereof.

CHANGES IN THE TRIBO-ELEMENTS

Ball Roughness

In order to verify the occurrence of wear on the ball during the tests, the surface roughness of the ball was verified for different sliding distances. Table 4 presents the values of the *Sq* roughness parameter for that.

TABLE 4

Variation of the ball surface roughness *Sq* for different sliding distances after contact with Al_2O_3 and B_4C particles

Sliding Distance, m	Al_2O_3	B_4C
0	0.05 ± 0.01	0.05 ± 0.01
48	0.06 ± 0.02	0.09 ± 0.02
96	0.06 ± 0.02	0.09 ± 0.02
192	0.07 ± 0.02	0.10 ± 0.01
287	0.07 ± 0.02	0.10 ± 0.01

Table 4 shows that some level of ball wear existed after the early stages, but after that, there was no significant change. Therefore, the wear of balls can be considered as irrelevant.

Particles

An analysis of the abrasive particles after the wear tests (192 and 383 m of sliding distance) was performed to evaluate the occurrence of changes or not in their morphologies and their relationship with the wear behavior of the material surface. Table 5 shows the values of d_{50} and SPQ parameters after wear tests.

Comparing the values of SPQ and d_{50} for the B_4C particles and Al_2O_3, it can be verified that statistically there were no significant changes to the parameters after 192 and 383 m of sliding distance. Consequently, the angularity and average size remain close to those of the supply state.

Because there was no variation in the medium diameter d_{50}, it can be said that the fine particle distribution did not increase, which would be a fact that could alter the angularity of the same. Therefore, it is suggested that the fragmentation should not have occurred during the process.

Another possibility for evaluating the effect of particles on the wear mode would be to apply a model that considers their mechanical properties. For that purpose, Pintaude[23] revised some models based on the elastic recovery of the worn surface to predict the abrasive wear rate. This author showed for different cases that the consideration of a combined elastic modulus (*Er*) is able to detect the effect of different abrasives acting on a surface. In this way, Table 6 shows the mechanical properties of the abrasives and D2 steel.

TABLE 5

Statistical parameters SPQ and d_{50} (%) to the B_4C and Al_2O_3 particles after tests

B_4C			
	SPQ		d_{50}, %
	$d_p > 7$ μm	$d_p < 7$ μm	
As a supply	0.34 ± 0.11	0.44 ± 0.14	6.5 ± 0.1
After 192 m (8 min)	0.34 ± 0.06	0.57 ± 0.11	6.4 ± 0.3
After 383 m (16 min)	0.43 ± 0.18	0.52 ± 0.14	6.5 ± 0.4
Al_2O_3			
	SPQ		d_{50} (%)
	$d_p > 7$ μm	$d_p < 7$ μm	
As a supply	0.44 ± 0.09	0.40 ± 0.11	6.7 ± 0.3
After 192 m (8 min)	0.47 ± 0.12	0.37 ± 0.14	6.6 ± 0.4
After 383 m (16 min)	0.49 ± 0.11	0.39 ± 0.10	6.6 ± 0.4

TABLE 6
Mechanical properties of the D2 steel and the particles

Abrasive Material	Elastic Modulus, E (GPa)	H (steel)/Er
D2 steel	207[27]	...
Al_2O_3[27]	379	0.046
B_4C	462[28]	0.043

Because the value of H/Er is practically the same for the combinations between Al_2O_3 and D2 steel and between B_4C and D2 steel, the effect of the mechanical properties of abrasives was insignificant to explain the differences in the wear coefficients produced by them.

NUMBER OF ACTIVE PARTICLES

Figure 7 shows the number of active particles of B_4C and Al_2O_3 during the contact. For the calculation of the active particles, the average size d_{50} of the abrasive particles was considered. According to figure 7, it is observed that the number of B_4C particles continues to increase gradually with an increase in the sliding distance, whereas the number of Al_2O_3 particles presents a less considerable increase. This behavior justifies the wear coefficient values observed in figure 4, in which B_4C particles were shown to have higher abrasivity on the material surface.

It is clear from figure 7 that the transitions between the transient and steady-state regimes are well detected by significant changes in the slopes of curves for both abrasives. This means that the number of active particles in the contact can explain the different behaviors of abrasives along testing time. It is out of our scope to investigate the reasons for these behaviors, which can be associated with the physicochemical properties of particles. For example, in the mechanical-chemical polishing, the interfacial resistance is able to change the process efficiency.[24] According to Gopal and Talbot,[25] the zeta potential of the solution has a greater influence on the slurry behavior. Changes of the suspension liquid can control the zeta potential such as pH, temperature, ionic strength, and ionic species. These factors suggest changes in the effective particle cluster size (formation of clusters). The values of zeta potential to the applicable solutions were measured, and any significant differences were observed (zeta potential [mV] to Al_2O_3 is −23.67 and to B_4C is −22.86). The pH of the suspensions was measured, 7.71 to Al_2O_3 and 6.12 to B_4C. For Al_2O_3, a solution with pH < 8 (below the isoelectric point) indicates that there are no changes in colloid stability.[25] For the B_4C, there are no changes in mean particle size in the pH range of 3 to 10, according to Varga, Csempesz, and Záray,[26] which indicates a stable slurry, considering only pH variation.

FIG. 7
Number of active particles in the contact.

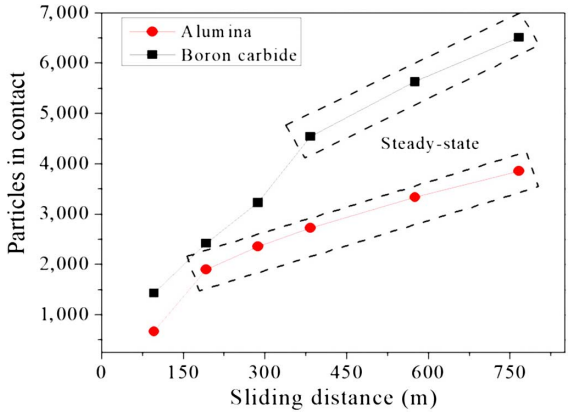

Another factor that can influence the number of active particles in contact, considering that the volume concentration and the diameter were the same for both abrasives, is the density of the particles. It is known that the density of the Al_2O_3 is greater than the B_4C; it can be supposed that the quantity of particles required for achieving the desired concentration (mass fraction) is lower as compared with the B_4C that has a lower density. According to obtained results, the wear rate was higher for the B_4C abrasive, which explains the number of active particles in contact, either by the density of the particles or by the diameter of the crater that allows a greater number of particles in the contact.

However, further developments can be made in this field for particle abrasivity determination.

Conclusions

This work presented a configuration for studying the particle abrasivity using the microscale abrasion test. The main difference between the recommendations of EN ISO 26424 (2016) and the variables used here is the high-level rotation speed. Using different abrasives, B_4C, and Al_2O_3 with similar particle distribution and particle shape, we can put forward the following conclusions:

- No changes of ball surface and particles during the micro-abrasive wear tests for both tested abrasives, which is very important for testing the particle abrasivity without any other interference of system.
- The steady-state wear regime was achieved at different sliding distances for each tested abrasive: at 192 m using Al_2O_3 and 383 m using B_4C. The grooving wear mode was associated with the steady-state regime, whereas a mixed mode of wear was observed during the initial stages.
- Particles of B_4C produced higher values of wear coefficient during the steady-state regime.
- The variations on the roughness parameter λ_q could be associated with the wear mode.
- The number of active particles in the contact increased with the sliding distance for both abrasives.
- A microscale abrasion test can be used for determining the particle abrasivity, although a significant number of particle characteristics should be taken into account for that purpose.

ACKNOWLEDGMENTS

The authors thank Robert Bosch Ltda for supplying the B_4C particles and Santana & Branco Ltda for supplying the Al_2O_3. G. Pintaude acknowledges CNPq for financial support through Process 308416/2017-1.

References

1. R. J. Plinninger and U. Restner, "Abrasiveness Testing, Quo Vadis?–A Commented Overview of Abrasiveness Testing Methods," *Geomechanics and Tunnelling* 1, no. 1 (February 2008): 61–70, https://doi.org/10.1002/geot.200800007
2. *Standard Test Method for Determination of Slurry Abrasivity (Miller Number) and Slurry Abrasion Response of Materials (SAR Number)* (Superseded), ASTM G75-01 (2015) (West Conshohocken, PA: ASTM International, approved November 1, 2015). https://doi.org/10.1520/G0075-01
3. *Standard Test Method for Laboratory Determination of Abrasiveness of Rock Using the CERCHAR Method*, ASTM D7625-10 (West Conshohocken, PA: ASTM International, approved May 15, 2010). https://doi.org/10.1520/D7625-10
4. G. R. Piazzetta, L. E. Lagoeiro, I. F. R. Figueira, M. A. G. Rabelo, and G. Pintaude, "Identification of Abrasion Regimes Based on Mechanisms of Wear on the Steel Stylus Used in the Cerchar Abrasiveness Test," *Wear* 410–411 (September 2018): 181–189, https://doi.org/10.1016/j.wear.2018.07.009
5. *Standard Test Method for Jaw Crusher Gouging Abrasion Test*, ASTM G81-97a (2018) (West Conshohocken, PA: ASTM International, approved November 15, 2018). https://doi.org/10.1520/G0081-97AR18
6. G. Pintaude and N. M. Bartalini, "Revisiting Gouging Abrasion Test for Jaw Crushers," *REM–International Engineering Journal* 71, no. 1 (January/March 2018): 111–115, https://doi.org/10.1590/0370-44672017710060
7. *Fine Ceramics (Advanced Ceramics, Advanced Technical Ceramics)—Determination of the Abrasion Resistance of Coatings by a Micro-Scale Abrasion Test*, ISO 26424:2008 (Geneva, Switzerland: International Organization for Standardization, approved November 1, 2008).
8. I. D. Marinescu, W. B. Rowe, B. Dimitrov, and H. Ohmori, *Tribology of Abrasive Machine Processes* (Waltham, MA: William Andrew Publishing, 2013), https://doi.org/10.1016/C2010-0-67070-2
9. K. L. Rutherford and I. M. Hutchings, "Theory and Application of a Micro-Scale Abrasive Wear Test," *Journal of Testing and Evaluation* 25, no. 2 (March 1997): 250–260, https://doi.org/10.1520/JTE11487J

10. D. A. Kelly and I. M. Hutchings, "A New Method for Measurement of Particle Abrasivity," *Wear* 250, nos. 1–12 (October 2001): 76–80, https://doi.org/10.1016/S0043-1648(01)00666-4
11. G. B. Stachowiak and G. W. Stachowiak, "The Effects of Particle Characteristics on Three-Body Abrasive Wear," *Wear* 249, nos. 3–4 (May 2001): 201–207, https://doi.org/10.1016/S0043-1648(01)00557-9
12. V. A. O. Gomez, M. C. S. de Macêdo, R. M. Souza, and C. Scandian, "Effect of Abrasive Particle Size Distribution on the Wear Rate and Wear Mode in Micro-Scale Abrasive Wear Tests," *Wear* 328–329 (April 2015): 563–568, https://doi.org/10.1016/j.wear.2015.03.015
13. M. G. Gee, A. Gant, I. M. Hutchings, R. Bethke, K. Schiffman, K. Van Acker, S. Poulat, Y. Gachon, and J. von Stebut, "Progress Towards Standardisation of Ball Cratering," *Wear* 255, nos. 1–6 (August/September 2003): 1–13, https://doi.org/10.1016/S0043-1648(03)00091-7
14. J. O. Bello and R. J. K. Wood, "Micro-Abrasion of Filled and Unfilled Polyamide 11 Coatings," *Wear* 258, nos. 1–4 (January 2005): 294–302, https://doi.org/10.1016/j.wear.2004.08.008
15. *Standard Test Method for Measuring Abrasion Using the Dry Sand/Rubber Wheel Apparatus*, ASTM G65-16e1 (West Conshohocken, PA: ASTM International, approved November 1, 2016). https://doi.org/10.1520/G0065-16E01
16. M. S. D. R. Coseglio, P. P. Moreira, H. L. Procópio, and G. Pintaude, "Analysis of the Efficiency of Hydroerosive Grinding without Renewal of Abrasive Particles," *Journal of Manufacturing Science and Engineering* 138, no. 3 (October 2016): 031007, https://doi.org/10.1115/1.4031053
17. G. Pintaude, "Characteristics of Abrasive Particles and Their Implications on Wear," in *New Tribological Ways* (London, UK: Intech, 2011), 117–130, https://doi.org/10.5772/14618
18. G. Pintaude and M. Coseglio, "Remarks on the Application of Two-Dimensional Shape Factors under Severe Wear Conditions," *Friction* 4, no. 1 (March 2016): 65–71, https://doi.org/10.1007/s40544-016-0105-y
19. K. Adachi and I. M. Hutchings, "Wear-Mode Mapping for the Micro-Scale Abrasion Test," *Wear* 255, nos. 1–6 (August/September 2003): 23–29, https://doi.org/10.1016/S0043-1648(03)00073-5
20. W. M. da Silva and J. D. B. de Mello, "Using Parallel Scratches to Simulate Abrasive Wear," *Wear* 267, no. 11 (October 2009): 1987–1997, https://doi.org/10.1016/j.wear.2009.06.005
21. D. N. Allsopp and I. M. Hutchings, "Micro-Scale Abrasion and Scratch Response of PVD Coatings at Elevated Temperatures," *Wear* 251, nos. 1–12 (October 2001): 1308–1314, https://doi.org/10.1016/S0043-1648(01)00755-4
22. R. C. Cozza, J. D. B. de Mello, D. K. Tanaka, and R. M. Souza, "Relationship between Test Severity and Wear Mode Transition in Micro-Abrasive Wear Tests," *Wear* 263, nos. 1–6 (September 2007): 111–116, https://doi.org/10.1016/j.wear.2007.01.099
23. G. Pintaude, "Introduction of the Ratio of the Hardness to the Reduced Elastic Modulus for Abrasion," in *Tribology: Fundamentals and Advancements* (London, UK: Intech, 2012), 217–230, https://doi.org/10.5772/55470
24. T. Sugimoto, S. Suda, and K. Kawahara, "Change in Slurry/Glass Interfacial Resistance by Chemical Mechanical Polishing," *MRS Advances* 2, no. 41 (2017): 2205–2210, https://doi.org/10.1557/adv.2017.335
25. T. Gopal and J. B. Talbot, "Effects of CMP Slurry Chemistry on the Zeta Potential of Alumina Abrasives," *Journal of the Electrochemical Society* 153, no. 7 (2006): G622–G625, https://doi.org/10.1149/1.2198128
26. I. Varga, F. Csempesz, and G. Záray, "Effect of pH of Aqueous Ceramic Suspensions on Colloidal Stability and Precision of Analytical Measurements Using Slurry Nebulization Inductively Coupled Plasma Atomic Emission Spectrometry," *Spectrochimica Acta–Part B: Atomic Spectroscopy* 51, no. 2 (January 1996): 253–259, https://doi.org/10.1016/0584-8547(95)01403-9
27. A. R. Franco Jr., G. Pintaúde, A. Sinatora, C. E. Pinedo, and A. P. Tschiptschin, "The Use of a Vickers Indenter in Depth Sensing Indentation for Measuring Elastic Modulus and Vickers Hardness," *Materials Research* 7, no. 3 (July/Sepetember 2004): 483–491, https://doi.org/10.1590/S1516-14392004000300018
28. V. Domnich, S. Reynaud, R. A. Haber, and M. Chhowalla, "Boron Carbide: Structure, Properties, and Stability under Stress," *Journal of the American Ceramic Society* 94, no. 11 (November 2011): 3605–3628, https://doi.org/10.1111/j.1551-2916.2011.04865.x